

MAE 271A Project: Calibration of an Accelerometer Using GPS Measurements

Aki A. Kono*

*Department of Mechanical and Aerospace Engineering,
University of California, Los Angeles, CA 90095, USA*

(Dated: December 14, 2022)

GPS-based calibration of unobservable accelerometer bias using Kalman filter algorithm applied to a linear dynamical system with Gaussian process is considered. The performance of Kalman filter is evaluated with transient estimation error convergence. The estimation error is simulated over the time period of 30 sec and averaged over $N = 3000$ Monte Carlo trials. The result shows that, on average, the bias is estimated with one sigma confidence intervals of $0.00 \pm 0.01 \text{m/sec}^2$ error after 10 sec and $0.0000 \pm 0.0025 \text{m/sec}^2$ error after 30 sec.

I. INTRODUCTION

An accelerometer is widely used in the guidance, navigation, and control of dynamical systems. The majority of accelerometers have a biased output. Biased error in acceleration is integrated and propagated to estimation errors in velocity and position. These errors and uncertainties grow over time if no calibration is performed. If the bias is deterministic, one-time calibration is sufficient to offset the error for the entire lifetime of the sensor. Accelerometer biases, however, are random, and therefore frequent calibration or estimation is desired. Estimation of unknown random bias can be achieved by additional measurements from GPS. Given GPS measurements, conditional probability distributions can be calculated using Bayes's rule with reduced estimation error and variance. Additional GPS measurements improve estimation, and the aim is to quantify how long it takes to achieve sufficient estimation accuracy with a given measurement frequency and sensor noises. Since the sensor noises are Gaussian distributed, the process is Gaussian and can be fully described by the time evolution of conditional mean and conditional variance. The minimum variance estimation is then given by choosing conditional mean as the estimate because the Gaussian distribution is symmetric and unimodal, therefore it gives the minimum variance.

The more general approach to the minimum variance estimation of a linear stochastic system was introduced by Kalman [1] in 1960. Kalman solved the minimum variance estimation or the least mean square error problem by applying the orthogonal projection lemma to a linear stochastic system in state space representation. This linear quadratic estimator is named the Kalman filter. Kalman filter outputs conditional mean estimates when the process is Gaussian, which is the best linear estimator and is just one particular case of many other minimum variance estimation problems where Kalman filter can be applied.

Here, Kalman filter, or the best linear estimator with minimum variance, is implemented to estimate accelerometer bias. Hence, the performance of the Kalman filter or the convergence rate of estimation error depends only on the sensor measurement accuracy and frequency. Given measurement error specifications of GPS and accelerometer, this report quantifies the error convergence in estimating accelerometer bias using the optimal linear filter or Kalman filter applied on a Gaussian process.

II. THEORY AND ALGORITHM

In this section, the implementation of Kalman filter algorithm is explained.

A. SENSOR MODELS

Noises in accelerometer and GPS are assumed Gaussian which makes the process also Gaussian. The accelerometer a_c is modeled as

$$a_c(t_j) = a(t_j) + b_a + w(t_j) \quad (1)$$

* akisaitoh@g.ucla.edu

TABLE I. SENSOR SPECIFICATIONS

Sensors	Measurement	Specifications
Accelerometer	Acceleration	Frequency: 200[Hz]
		White Gaussian noise: $\mathcal{N}(0, (0.02[m/s^2])^2)$
		Time constant bias: $\mathcal{N}(0, (0.1[m/s^2])^2)$
GPS	Velocity	Frequency: 5[Hz]
		White Gaussian noise: $\mathcal{N}(0, (0.04[m/s])^2)$
		Random initial error: $\mathcal{N}(100, (1[m/s])^2)$
	Position	Frequency: 5[Hz]
		White Gaussian noise: $\mathcal{N}(0, (1[m])^2)$
		Random initial error: $\mathcal{N}(0, (10[m])^2)$

where b_a is a time constant accelerometer bias with known priori probability distribution $\mathcal{N}(0, (0.1[m/s^2])^2)$, and $w(t_j)$ is a white Gaussian noise added to each measurement at time t_j . The bias is modeled as constant over time during one realization but randomly chosen from known probability distribution of the bias errors. The GPS is modeled as

$$z_{1i} = x_i + \eta_{1i}$$

$$z_{2i} = v_i + \eta_{2i}$$

where x_i is a position, v_i is a velocity, and η_i and η_{2i} are additive, independent, white, zero-mean, Gaussian noises. The sampling rate of accelerometer and GPS are 200Hz and 5Hz respectively and are synchronized. Sensor measurement specifications are summarized in Table I.

B. SIMULATION MODEL AND ERROR DYNAMIC MODEL

The acceleration simulation model is defined to be the periodically time varying continuous function

$$a(t) = a \sin(\omega t) \quad (2)$$

where the amplitude $a = 10$ meters/sec² and by letting $\omega = 0.1$ the period is given by $2\pi/\omega = 62.8$ sec. The duration of the simulation is 30 sec. The simulation model or the truth model of position p , velocity v , and acceleration bias b are given by

$$\begin{aligned} v(t) &= v(0) + \frac{a}{\omega} - \frac{a}{\omega} \cos(\omega t) \\ p(t) &= p(0) + \left(v(0) + \frac{a}{\omega}\right) t - \frac{a}{\omega^2} \sin(\omega t) \end{aligned}$$

$$\begin{bmatrix} p(t) \\ v(t) \\ b(t) \end{bmatrix} = \begin{bmatrix} 1 & t & 0 \\ 0 & 1 & 0 \\ 0 & 0 & 1 \end{bmatrix} \begin{bmatrix} p(0) \\ v(0) \\ b(0) \end{bmatrix} + \begin{bmatrix} \frac{a}{\omega} t - \frac{a}{\omega^2} \sin(\omega t) \\ \frac{a}{\omega} (1 - \cos(\omega t)) \\ 0 \end{bmatrix}$$

To obtain system of equations in the discrete time equivalent form, the first and second integration of true acceleration profile (2) is approximated with Euler method in difference equation form

$$\begin{aligned} v_E(t_{j+1}) &= v_E(t_j) + a(t_j) \Delta t \\ p_E(t_{j+1}) &= p_E(t_j) + v_E(t_j) \Delta t + a(t_j) \frac{\Delta t^2}{2} \end{aligned} \quad (3)$$

Similarly, the first and second integration of accelerometer model gives

$$\begin{aligned} v_c(t_{j+1}) &= v_c(t_j) + a_c(t_j) \Delta t \\ p_c(t_{j+1}) &= p_c(t_j) + v_c(t_j) \Delta t + a_c(t_j) \frac{\Delta t^2}{2} \end{aligned} \quad (4)$$

Subtracting equation (4) from (3) and substituting (1) yields

$$\underbrace{\begin{bmatrix} \delta p_E(t_{j+1}) \\ \delta v_E(t_{j+1}) \\ b(t_{j+1}) \end{bmatrix}}_{\delta(t_{j+1})} = \underbrace{\begin{bmatrix} 1 & \Delta t & -\frac{\Delta t^2}{2} \\ 0 & 1 & -\Delta t \\ 0 & 0 & 1 \end{bmatrix}}_{\Phi} \underbrace{\begin{bmatrix} \delta p_E(t_j) \\ \delta v_E(t_j) \\ b(t_j) \end{bmatrix}}_{\delta x(t_j)} - \underbrace{\begin{bmatrix} \frac{\Delta t^2}{2} \\ \Delta t \\ 0 \end{bmatrix}}_{\Gamma} w(t_j) \quad (5)$$

where

$$\begin{aligned} \delta p_E(t_0) &= p_E(t_0) - p_c(t_0) \sim N(0, (10[m])^2) \\ \delta v_E(t_0) &= v_E(t_0) - v_c(t_0) \sim N(0, (1[m/s])^2) \\ E[w(t_j)] &= 0, E[w(t_j)w(t_\ell)^T] = W\delta_{j,\ell} \\ b(0) &\sim N(0, (0.1[m/s^2])^2) \end{aligned}$$

State variables are chosen such that stochastic discrete time system is independent of acceleration profile and independent of Euler method approximation error. Similarly, measurement equations expressed with state variables are given by

$$\underbrace{\begin{bmatrix} \delta z^p(t_i) \\ \delta z^v(t_i) \end{bmatrix}}_{\delta z(t_i)} = \underbrace{\begin{bmatrix} 1 & 0 & 0 \\ 0 & 1 & 0 \end{bmatrix}}_H \underbrace{\begin{bmatrix} \delta p(t_i) \\ \delta v(t_i) \\ b(t_i) \end{bmatrix}}_{\delta x(t_i)} + \underbrace{\begin{bmatrix} \eta^p(t_i) \\ \eta^v(t_i) \end{bmatrix}}_{v(t_i)} \quad (6)$$

C. KALMAN FILTER ALGORITHM

Kalman filter is then applied to the system of linear equations in state-space representation form given by (5) and (6) or in simplified form

$$\begin{aligned} \delta x(t_{j+1}) &= \Phi \delta x(t_j) - \Gamma w(t_j) \\ \delta z(t_i) &= H \delta x(t_i) + v(t_i) \end{aligned}$$

where discrete time steps Δt_j and Δt_i are 0.005 sec and 0.2 sec, respectively. The GPS measurements are assumed to be first available at $t_j = t_i = 0.02$ sec and synchronized for every $40 \cdot \Delta t_j$ sec. The system dynamics are unstable since $|\Phi| = 1.73 > 1$ when $\Delta t = \Delta t_j$ and $|\Phi| = 1.75 > 1$ when $\Delta t = \Delta t_i$. Kalman filter recursive process is illustrated in Figure 1. Given the initial state error $\widehat{\delta x_0}$ and covariance matrix P_0 at $k = 0$, stochastic process starts from propagating initial error and variance forward in one time step with priori conditional mean and variance equations

$$\begin{aligned} \overline{\delta x_{k+1}} &= \Phi \widehat{\delta x_k} \\ M_{k+1} &= \Phi P_k \Phi^T + \Gamma W_k \Gamma^T \end{aligned}$$

When GPS measurements are available, measurement inputs δz_{k+1} are given, and estimation error and variance are calculated with posteriori conditional mean and variance equations

$$\begin{aligned} \widehat{\delta x_{k+1}} &= \overline{\delta x_{k+1}} + P_{k+1} H^T V_{k+1}^{-1} (\delta z_{k+1} - H \overline{\delta x_{k+1}}) \\ P_{k+1} &= (M_{k+1}^{-1} + H^T V_{k+1}^{-1} H)^{-1} \end{aligned}$$

When GPS measurements are not available, error and variance are propagated with priori conditional mean and variance equations. The recursive process is continued until 30.005 sec is reached. This completes one realization of estimation error dynamics.

III. RESULTS AND PERFORMANCE

The performance of Kalman filter algorithm in estimating the accelerometer bias, velocity, and position, are illustrated in Figure 2, 3, and 4, respectively with the estimation error convergence plotted against time. These figures

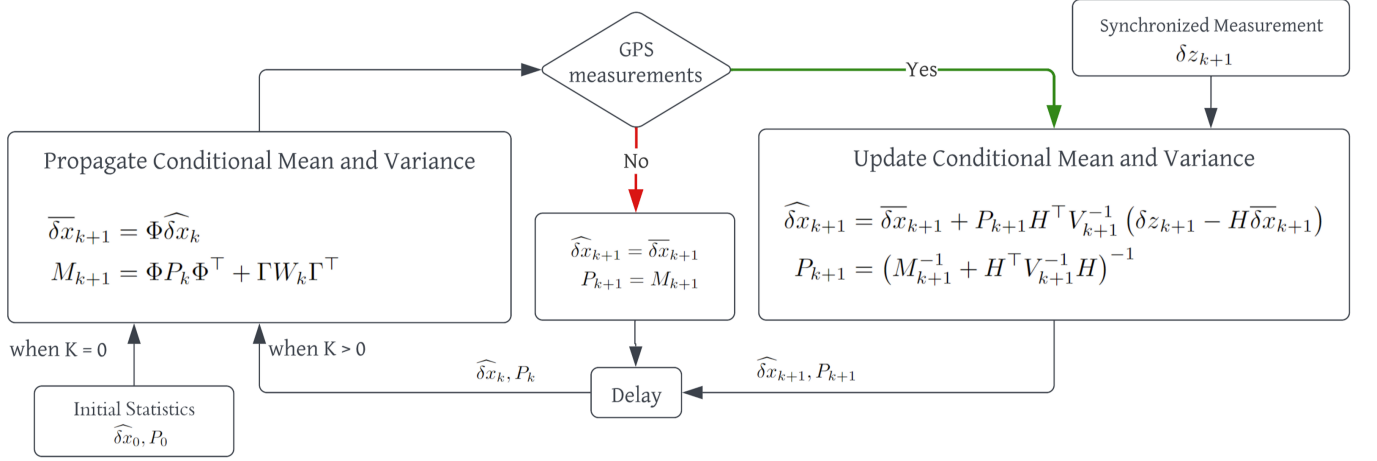


FIG. 1. Kalman filtering algorithm.

are the results of $N = 3000$ Monte Carlo simulations. Red solid line in each figure is the one sigma bound of variance averaged over the 3000 realizations. Green dots are the estimates averaged over the 3000 realizations. Plotted in orange dots are posteriori estimates and blue dots are priori estimates of a realization with the largest bias in acceleration for Figure 2, the largest initial error in velocity for Figure 3, and the largest initial error in position for Figure 4. Yellow solid line in each figure is the signal noise of these worst case realizations. The multiple dots shown in the bottom plot in each figure is a random 20 realizations of estimates.

One sigma bound of estimation of acceleration bias reaches ± 0.01 m/sec² after 10 sec and ± 0.0025 m/sec² after 30 sec. One sigma bound of velocity estimates reaches ± 0.05 m/sec after 10 sec and ± 0.025 m/sec after 30 sec. One sigma bound of position estimates reaches ± 0.2 m after 5 sec and stays the same after 30 sec. These one sigma bounds obtained from the covariance matrix averaged over $N = 3000$ can be compared with the error variance from one realization shown in Figure 5 in which each element of the covariance matrix is plotted for the worst acceleration bias case. The blue, orange, and green lines represent the position, velocity, and acceleration bias variance respectively, and others are off-diagonal elements.

These results from Kalman filter algorithm is verified by illustrating the error variance computed to form the Kalman gain $P(t_i)$ is close to the actual error variance obtained from $N = 3000$ Monte Carlo simulation runs P^{ave} where

$$P^{ave}(t_i) = \frac{1}{N_{ave} - 1} \sum_{l=1}^{N_{ave}} [e^l(t_i) - e^{ave}(t_i)] [e^l(t_i) - e^{ave}(t_i)]^T$$

and

$$e^{ave}(t_i) = \frac{1}{N_{ave}} \sum_{l=1}^{N_{ave}} e^l(t_i)$$

It is expected that $e^{ave}(t_i) \approx 0$ for all $t_i \in [0, 30]$. Figure 6 shows averaged errors are close to zero for all t_i . Therefore, $N = 3000$ is considered a statistically sufficient number of samples to generalize the results.

The element-wise comparison between above mentioned covariance matrices $P^{ave}(t_i)$ and $P(t_i)$ are shown in Figure 7 and $P^{ave}(t_i) - P(t_i) \approx 0$ is shown in Figure 8. Similarly, the orthogonality of estimate errors and estimates is given as $\frac{1}{N_{ave}} \sum_{l=1}^{N_{ave}} [e^l(t_i) - e^{ave}(t_i)] \hat{x}(t_i)^T \approx 0 \forall t_i$ and is plotted as a function of time in Figure 9. Finally, the correlation of residuals is checked between two selected time steps

$$\frac{1}{N_{ave}} \sum_{l=1}^{N_{ave}} r^l(t_i)^l(t_m)^T = \begin{cases} \begin{bmatrix} -0.406 & 0.0168 \\ 0.0091 & 0.0388 \end{bmatrix} & \text{for } t_m = 0 \text{ sec}, t_i = 0.2 \text{ sec} \\ \begin{bmatrix} -0.0899 & 0.00833 \\ 0.000487 & 0.00833 \end{bmatrix} & \text{for } t_m = 0 \text{ sec}, t_i = 30 \text{ sec} \end{cases}$$

The above checked correlations are near zero for all evaluated values as expected. This results verify that Kalman filter is implemented appropriately.

IV. CONCLUSIONS

The Kalman filter is evaluated with error convergence in estimating unobservable accelerometer bias. One sigma confidence interval of $0.00 \pm 0.01 \text{m/sec}^2$ error after 10 sec and $0.0000 \pm 0.0025 \text{m/sec}^2$ error after 30 sec are observed from numerical simulation. The implementation of the Kalman filter algorithm is verified with its orthogonality properties.

-
- [1] R. E. Kalman, A new approach to linear filtering and prediction problems, Journal of Basic Engineering **82**, 35 (1960).

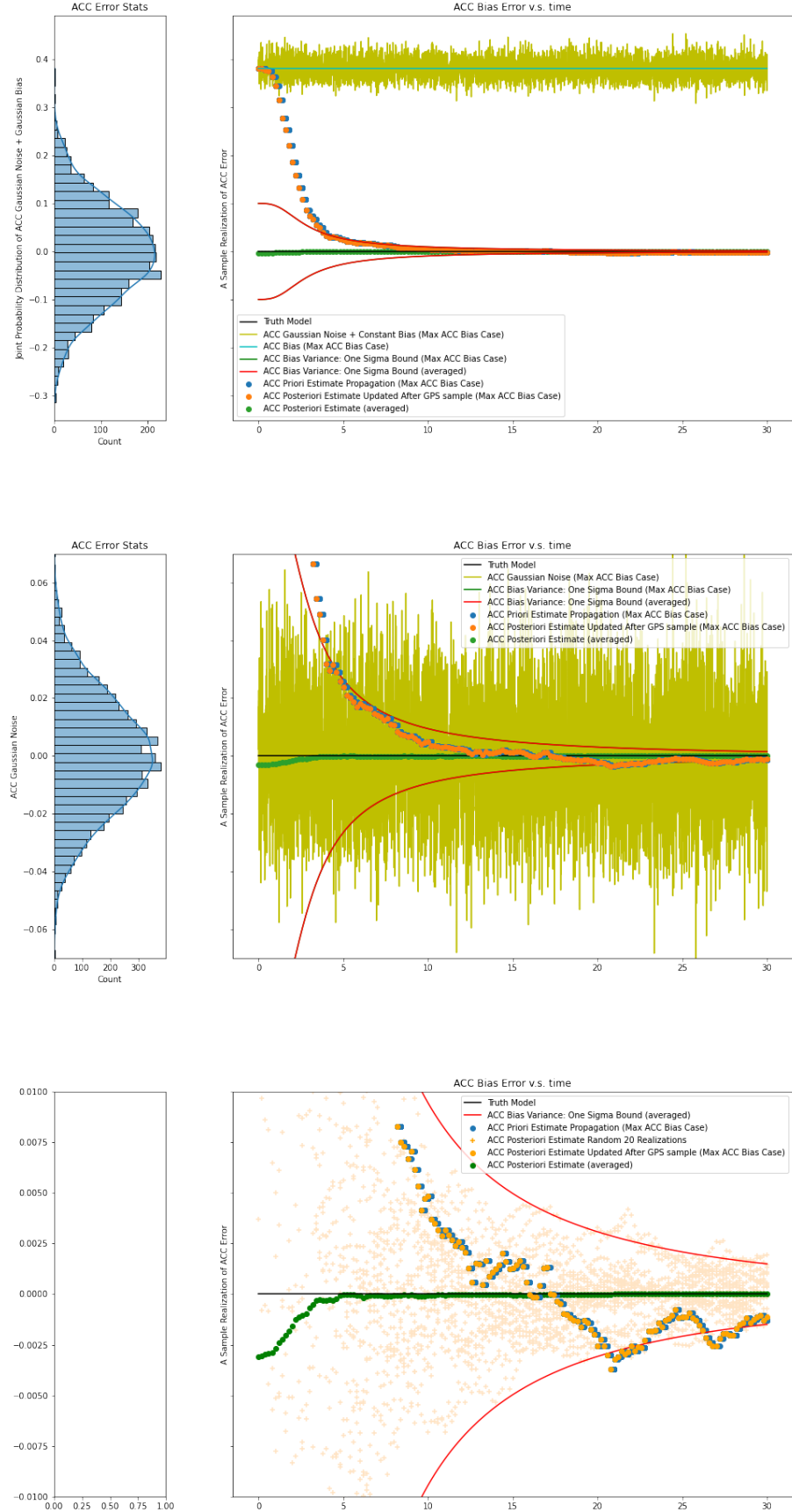


FIG. 2. Convergence of error and uncertainty over time against noise (Acceleration). TOP: with statistics of bias and noise. MIDDLE: with statistics of noise. BOTTOM: with 20 random realizations.

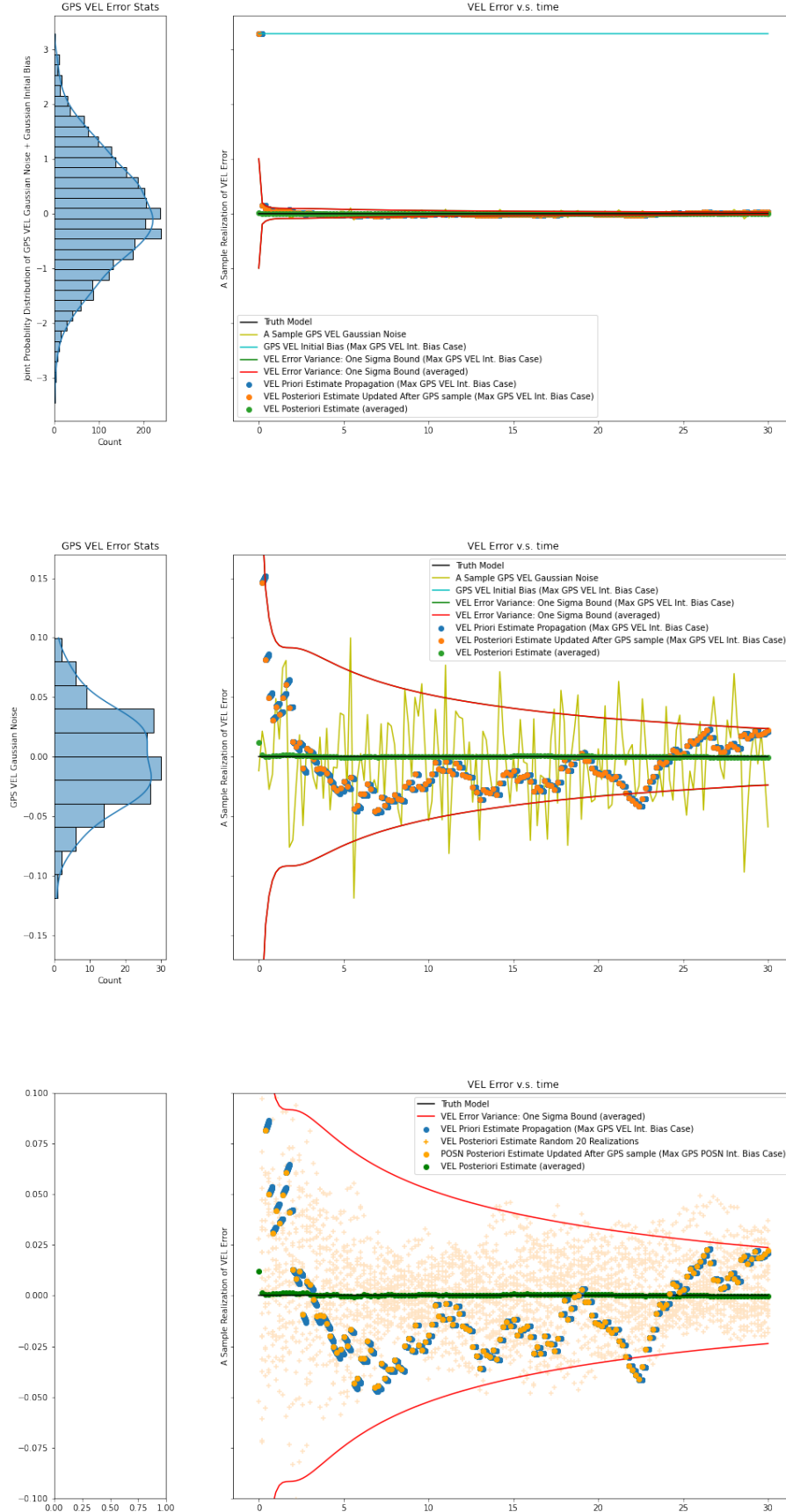


FIG. 3. Convergence of error and uncertainty over time against noise (Velocity). TOP: with statistics of initial bias and noise. MIDDLE: with statistics of noise. BOTTOM: with 20 random realizations.

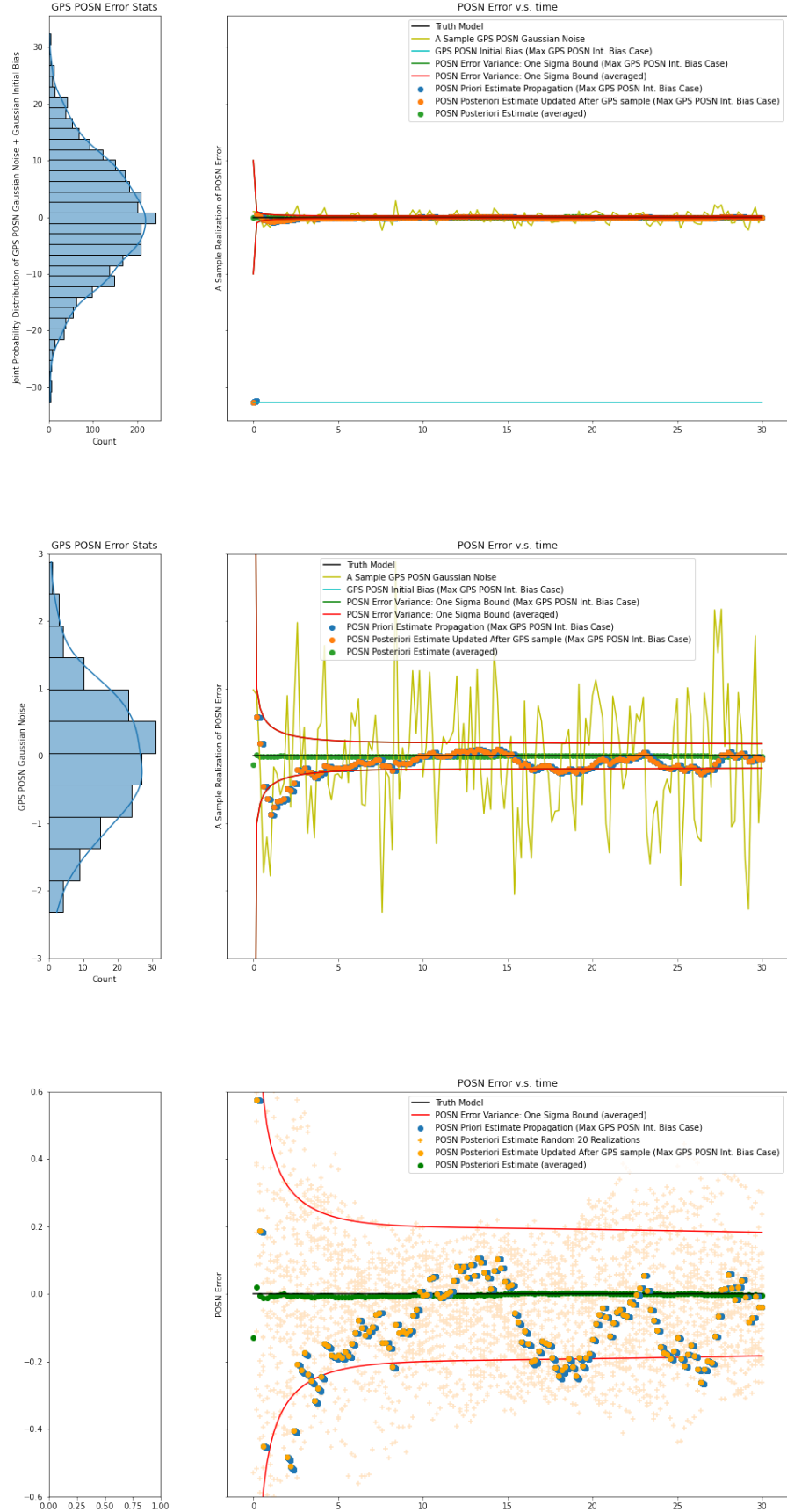


FIG. 4. Convergence of error and uncertainty over time against noise (Position). TOP: with statistics of initial bias and noise. MIDDLE: with statistics of noise. BOTTOM: with 20 random realizations.

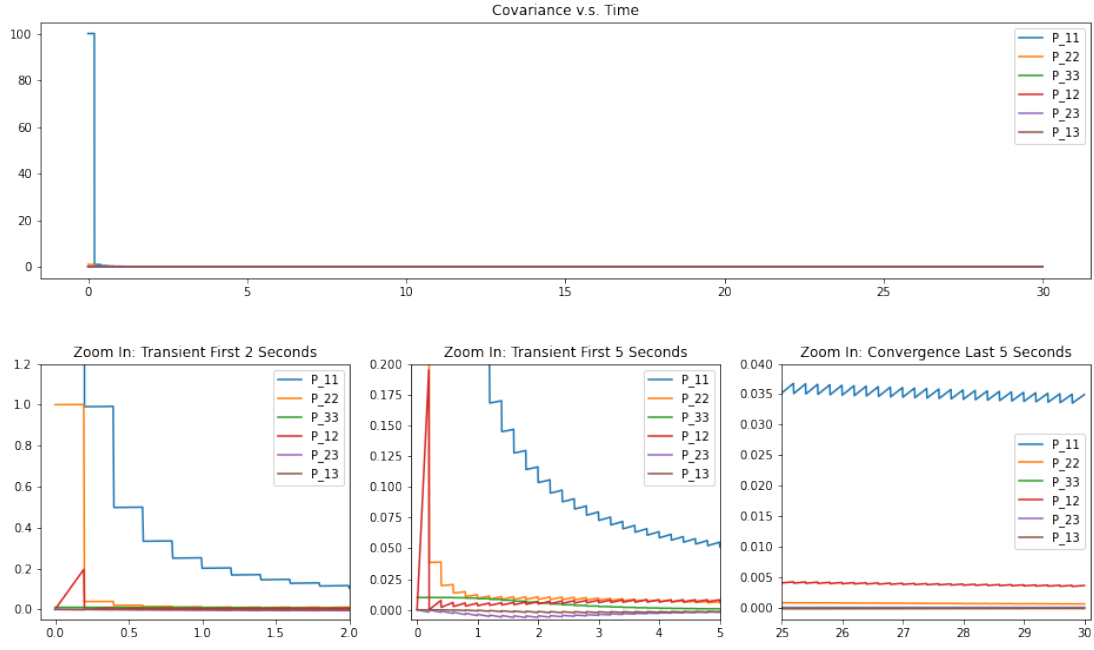


FIG. 5. Diagonal and off-diagonal elements of covariance matrix obtained from the largest acceleration bias case.

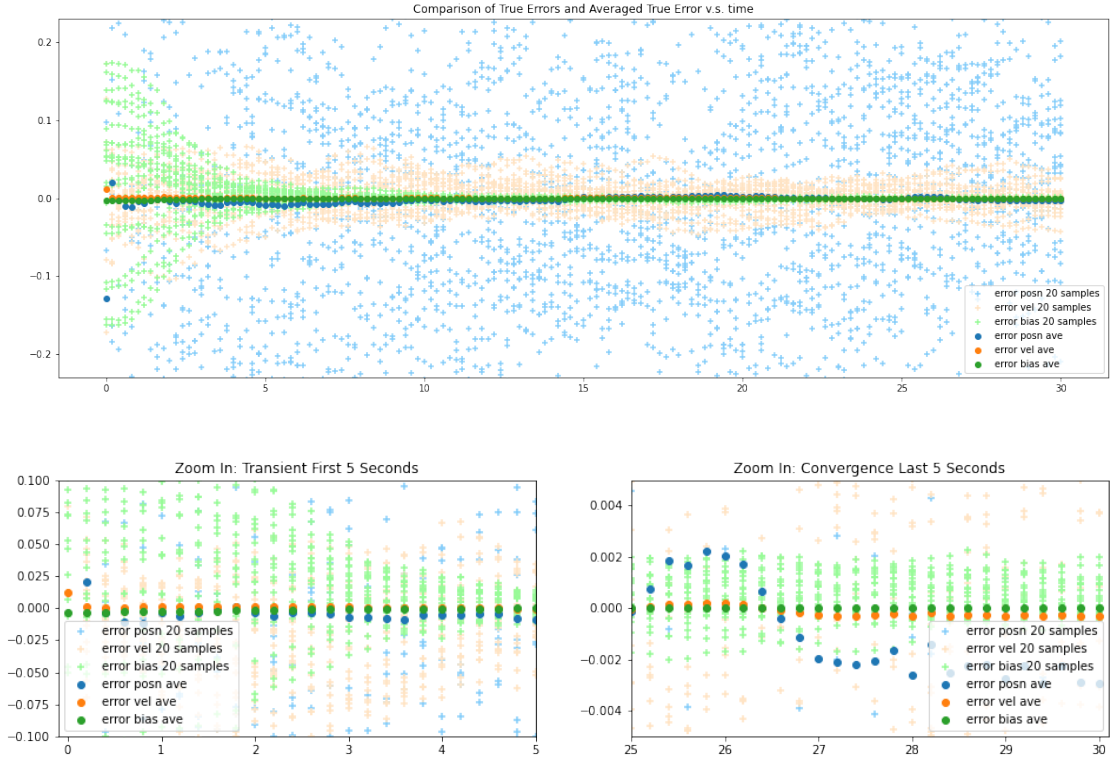


FIG. 6. Comparison of errors and averaged error ($N=3000$)

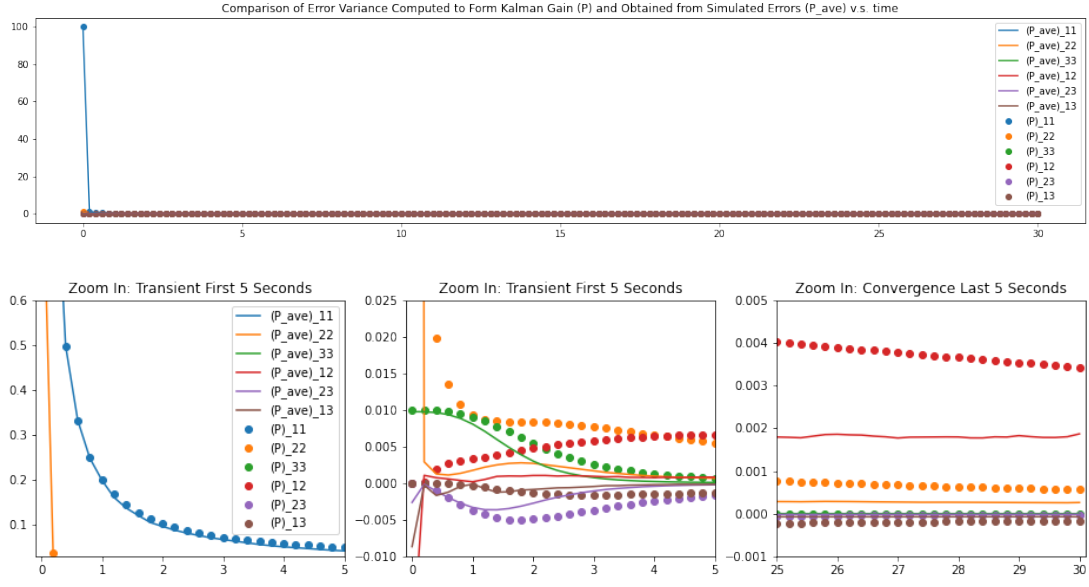


FIG. 7. Comparison of error variance computed to form Kalman gain and variance obtained from simulated errors.

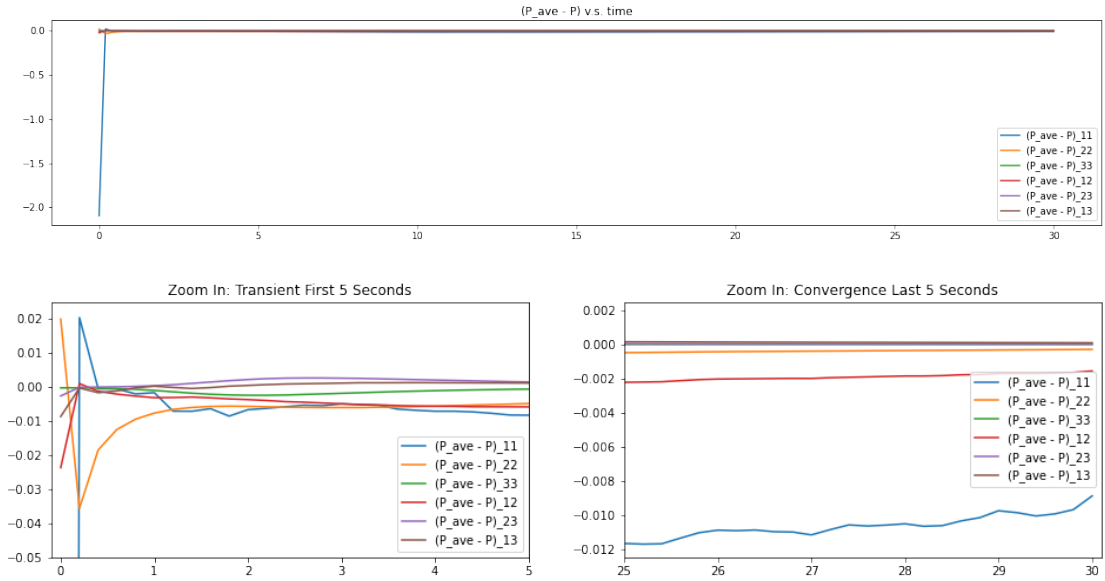


FIG. 8. Covariance from Kalman Filter subtracted from covariance calculated from ground-truth errors and estimated errors.

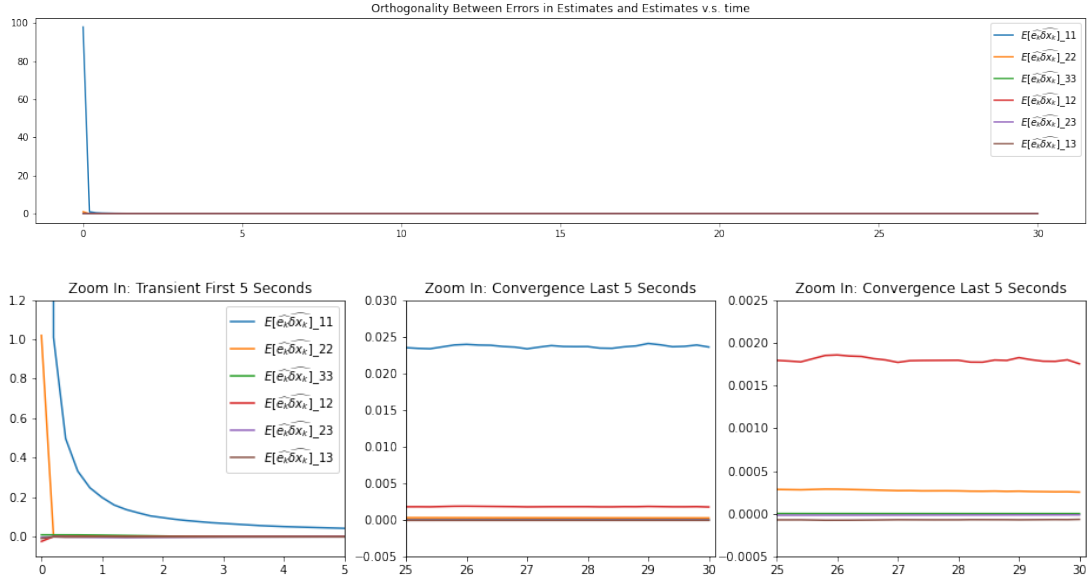


FIG. 9. Orthogonality of estimate errors and estimates.